An updated model for nitrate uptake modelling in plants. II. Assessment of active root involvement in nitrate uptake based on integrated root system age: measured versus modelled outputs

Philippe Malagoli, Erwan Le Deunff

Annals of Botany **113**: 1007–1019, 2014
doi:10.1093/aob/mcu022, available online at www.aob.oxfordjournals.org

ANNALS OF BOTANY
Founded 1887

An updated model for nitrate uptake modelling in plants. II. Assessment of active root involvement in nitrate uptake based on integrated root system age: measured versus modelled outputs

Philippe Malagoli[1,2,*] and Erwan Le Deunff[3,4]

[1]*Clermont Universités, Université Blaise Pascal, UMR 547 PIAF, BP 10448, F-63000 Clermont Ferrand, France,* [2]*INRA, UMR 547 PIAF, F-63100 Clermont Ferrand, France,* [3]*Université de Caen Basse-Normandie, UMR EVA, F-14032 Caen cedex, France and* [4]*INRA, UMR 950, Écophysiologie Végétale & Agronomie Nutritions NCS, F-14032 Caen cedex, France*
** For correspondence. E-mail Philippe.MALAGOLI@univ-bpclermont.fr*

Received: 14 November 2013 Returned for revision: 7 January 2014 Accepted: 21 January 2014 Published electronically: 6 April 2014

• *Background and Aims* An updated version of a mechanistic structural–functional model was developed to predict nitrogen (N) uptake throughout the growth cycle by a crop of winter oilseed rape, *Brassica napus*, grown under field conditions.
• *Methods* The functional component of the model derives from a revisited conceptual framework that combines the thermodynamic Flow–Force interpretation of nitrate uptake isotherms and environmental and *in planta* effects on nitrate influx. Estimation of the root biomass (structural component) is based upon a combination of root mapping along the soil depth profile in the field and a relationship between the specific root length and external nitrate concentration. The root biomass contributing actively to N uptake was determined by introduction of an integrated root system age that allows assignment of a root absorption capacity at a specific age of the root.
• *Key Results* Simulations were well matched to measured data of N taken up under field conditions for three levels of N fertilization. The model outputs indicated that the two topsoil layers (0–30 and 30–60 cm) contained 75–88 % of the total root length and biomass, and accounted for 90–95 % of N taken up at harvest.
• *Conclusions* This conceptual framework provides a model of nitrate uptake that is able to respond to external nitrate fluctuations at both functional and structural levels.

Key words: Nitrate, N uptake regulation, Flow–Force interpretation, nitrogen uptake efficiency, root development, root longevity, functional–structural plant model, N uptake modelling, *Brassica napus*.

INTRODUCTION

An improvement in structural–functional models of N uptake is becoming increasingly important for agriculture to optimize management of N fertilization and, ultimately, to match the worldwide increase in food demand with changes in climate variables such as the amounts and distribution of precipitation, temperature levels and CO_2 concentrations (Brouder and Volenec, 2008; Gregory and George, 2011). These models will be helpful tools to better understand interactions between root development and root N uptake for plant growth to improve nitrogen- and water-use efficiency (NUE and WUE) and propose different scenarios for screening new plant ideotypes based on nitrate uptake and/or root structure performances (King *et al.*, 2003; Good *et al.*, 2004; Lynch, 2007; Herder *et al.*, 2010). However, a simplified and operational modelling approach of nitrate uptake regulation has been lacking because of the integration inconsistency of nitrate influx regulation by endogenous and exogenous factors acting over different space- and time-scales. To reduce this inconsistency, a new conceptual N-uptake model based on the cross-combination between the Flow–Force theory of ion uptake isotherms (Thellier, 1970, 1973, 2012; Thellier *et al.*, 2009) and the effects of environmental and endogenous (i.e. *in planta*) factors on the regulation of nitrate influx has been built. This new conceptual framework is presented in a companion paper (Le Deunff and Malagoli, 2014). Comparison of the design and construction of this version of the updated model to the previous one (Malagoli *et al.*, 2004, 2008) is illustrated in Fig. 1. The new formalism assumes the existence of a single root catalytic structure composed of a complex of nitrate transporters (CNT) distributed along the root radius under a series and/or parallel arrangement within the different root cell layers. In addition, this new conceptual framework was strengthened with a more accurate prediction of root system growth (the structural component of the model) based upon (1) field mapping of root development, (2) conversion to the root length, (3) conversion to root biomass through the relationship between specific root length (SRL) and nitrate concentrations obtained under controlled conditions, and (4) decreasing nitrate uptake along the root axes with root age (Gao *et al.*, 1998). This allows a cross-combination between the effects of nitrate concentrations on environmental [photosynthetically active radiation (PAR) and temperatures] and *in planta* factors (day/night and ontogenesis cycles) to propose a novel model that predicts N acquisition by plants based upon both the functioning of nitrate transporters and the root biomass in different soil layers.

At a structural level, most N uptake models focus on simulating root biomass or length (i.e. root structure) during the growth cycle along the soil depth profile. Under field conditions,

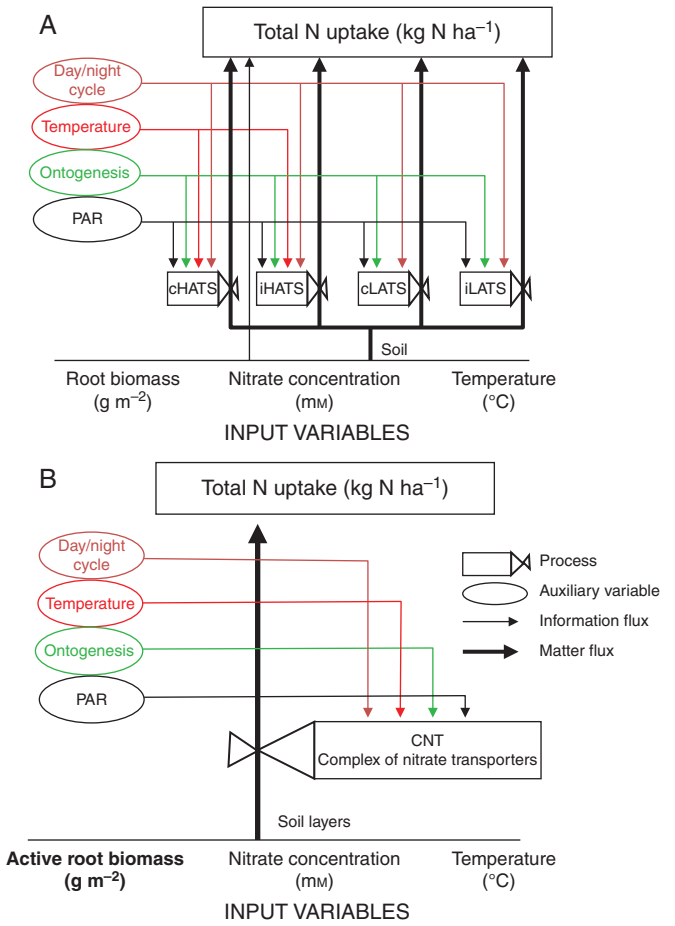

FIG. 1. Conceptual framework to model nitrate uptake derived from (A) Enzyme–Substrate and (B) Flow–Force theories. Inputs and outputs are provided from the INRA winter oilseed rape database (http://www-egc.grignon.inra.fr/applis/ecobilan/eco.html). Auxiliary variables correspond to HATS and LATS (high and low affinity transport systems) (A) or CNT (B) response curves to environmental factors.

parameters characterizing dynamic root growth in soil can be estimated through different methods such as root mapping, endoscopic analyses and image analyses of soil cores (Newman, 1966; Maertens, 1987; Gabrielle *et al.*, 1998*a*, *b*; Liu *et al.*, 2010, 2011*a*, *b*; Gan *et al.*, 2011). So far, this has resulted in modelling of root development along the growth cycle by using the formalism of Gerwitz and Page (1974) (Petersen *et al.*, 1995; Gabrielle *et al.*, 1998*a*, *b*; King *et al.*, 2003; Albert, 2008). Use of this formalism shows that more than 80–90 % of the biomass or root length of different crop species is found in the first 0–40 cm soil layer by the end of the growing period (Barraclough, 1989*a*, *b*; King *et al.*, 2003; Ma *et al.*, 2008; Liu *et al.*, 2011*b*). In canola and cauliflower, root length estimation at the end of the growth cycle revealed no difference between high and low levels of N fertilization along the whole soil profile (Petersen *et al.*, 1995; Gabrielle *et al.*, 1998*a*; Gosse *et al.*, 1999; Kage *et al.*, 2000; Albert, 2008). This is clearly in contradiction to the well-established physiological effects of nitrate on root development observed under controlled conditions (Drew and Saker, 1975; Scheible *et al.*, 1997; Zhang *et al.*, 1999). One explanation of this discrepancy is that in a biannual crop species such as winter oilseed rape, root growth occurs predominantly during autumn and winter and most of the root system is set before the bolting period and subsequent N fertilization occurring before the flowering stage (Barraclough, 1989*b*).

The main hypotheses used to build this model were as follows: (1) each different soil layer considered is homogeneous and isotropic for nitrate ions with respect to soil characteristics, (2) the sole nitrogen source is nitrate, (3) active transport for nitrate uptake (i.e. nitrate influx measured during 5 min) occurs at the root surface and can be described by the Flow–Force relationship, (4) N-uptake regulation acting throughout the day–night and ontogenetic cycles is the sum of the Flow–Force relationship describing hourly nitrate-dependent isotherms, (5) the combination of mass flow and diffusion providing nitrate to the root is not limiting because the soil water content values are close to field capacity and hardly change, (6) nitrate influx depends on environmental factors such as temperature and PAR that modify the $I([NO_3^-]_i)_i$ value of nitrate influx [see (1) in Materials and methods], (7) nitrogen uptake decreases along the root axes according to root age (Warncke and Barber, 1974; Bhat *et al.*, 1979; Gao *et al.*, 1998; Eissenstat and Volder, 2005; Chen and Brassard, 2013), and (8) no root competition for nutrient uptake nor effects of biotic constraints are taken into account.

In this paper, the model is evaluated for its capacity to simulate satisfactorily the dynamics of root N acquisition rate during the whole growth cycle. First, we propose an improved method to estimate active absorbing root biomass in the different soil layers during the whole growth cycle (root structural component of the model). Then, model outputs are compared with measured N taken up by winter oilseed rape with three levels of N fertilization. Outputs of the model and associated physiological interpretations are discussed.

MATERIALS AND METHODS

Nitrate exported by plants every i degree-day (°Cd) in the model is expressed in N kg ha^{-1} and is derived from the following equation of nitrate influx:

$$N_i = I\left(\left[NO_3^-\right]_i\right)_i \times U_i \times \left(\text{active absorbing root dry weight}\right)_i \times 10\,000 \quad (1)$$

where N_i exported corresponds to N taken up by the crop (kg ha^{-1}), $I([NO_3^-]_i)_i$ is the nitrate influx (kg N g^{-1} root d. wt °Cd^{-1}) according to soil nitrate concentration ($[NO_3^-]_i$) at the ith °Cd and U_i (unitless; ranging from 0 to 1) is a uniformization factor used to normalize heterogeneity of influx measurements in response to the studied factors (temperature, PAR, ontogenesis and day–night cycles) among the different laboratory experiments. U_i has been extensively detailed in our companion paper (Le Deunff and Malagoli, 2014). Briefly $I([NO_3^-]_i)_i$ is modelled through the Flow–Force theory and U_i allows application of environmental (temperature and radiation) and endogenous (day/night and ontogenesis) effects on nitrate influx according to soil external nitrate concentrations. The active absorbing root dry weight (DW) is expressed as g m^{-2} and the factor 10 000 is used to convert units from m^2 to ha. The absorbing root dry weight is an input variable necessary to run the

model, and it is dependent on both calculation of total fine-root dry weight provided by field data and the age of the root system throughout the growth cycle. The calculation is detailed in the section below.

Calculations of the root biomass from total fine-root length as a function of soil depth and time

Total fine-root length actively contributes to nitrate uptake and was specifically estimated from field data. The calculation was based upon the root distribution profile in the soil from the soil surface to rooting depth along the growth cycle according to Gabrielle *et al.* (1998*a*, *b*). After digging a trench between rows, a grid with squares (1 × 1 cm) was laid along the soil profile. Appearance or non-appearance of root tips in each square allowed us to calculate a percentage (% root impact) of grid filling and a subsequent root mapping. Those were converted to root length density (RLD_i) for each *i*th °Cd in cm of root cm^{-3} soil according to the following relationship:

$$RLD_i = \left(\%\ \text{root impact}\right)_i \times RLD_{max} \quad (2)$$

where RLD_{max} is the maximum RLD observed in the 0–30 cm soil layer at the end of the growth cycle. The RLD_{max} value used by Gabrielle *et al.* (1998*a*, *b*) was 5 cm cm^{-3}. This conversion value was established from the field study of Petersen *et al.* (1995). However, in this study the averaged RLD within the first layer of 0–30 cm is not around 5 but 3 cm cm^{-3} at the end of the growth cycle. Hence, this value was used to estimate root lengths for the three levels of fertilization (N0, 0 kg N ha^{-1}; N1, 135 kg N ha^{-1}; N2, 272 kg N ha^{-1}) as a function of soil depth during the whole growth cycle (Fig. 2). The following equation was used to calculate the total fine-root DW from the RLD values derived from the per cent root impact given by the INRA oilseed rape database (http://www-egc.grignon.inra.fr/applis/ecobilan/eco.html) in the different soil layers of 10 cm height:

$$DW_{root,i} = RLD_i \times SRL\left(\left[NO_3^-\right]_i\right)_i \times 100 \quad (3)$$

where $DW_{root,i}$ is root biomass (in g m^{-2}), RLD_i is root length density (cm cm^{-3}), SRL is specific root length (mg cm^{-1} root) according to soil nitrate concentration ($[NO_3^-]_i$)$_i$ and the factor 100 [=0·001 (to convert root mg to g) × 10 (to extend a soil layer of 1 cm height to 10 cm) × 10 000 (to extend from a 1-cm^2 to 1-m^2 area)] allows the conversion of mg cm^{-3} to g m^{-2} in a soil layer of 10 cm height. The fine-root dry weight estimation was calculated from a response curve of SRL to soil external nitrate concentrations. Changes in SRL with soil nitrate availability were monitored from two extra experiments on 7-d-old seedlings grown on agar plates with a homogeneous and broad range of nitrate concentrations from 0·05 to 20 mM according to Le Ny *et al.* (2013). Then, the equation of the SRL response curve to nitrate concentrations (Fig. 2) was used to calculate the root dry matter from the changes in soil nitrate concentrations and the total RLD estimated in the different soil layers by combining eqns (2) and (3). The estimated DW_{root} values for the different soil layers of 10 cm height until 1·2 m soil depth were then summed to get DW_{root} for soil layers of 30 cm height (L1, 0–30 cm; L2, 30–60 cm; L3, 60–90 cm; L4, 90–120 cm).

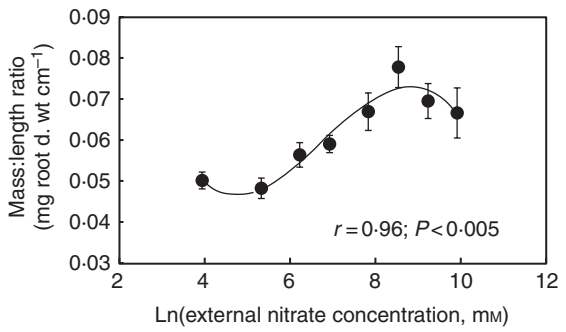

FIG. 2. Effect of external nitrate concentrations on variations in the specific root length in 7-d-old winter oilseed rape (*Brassica napus* 'Capitol') seedlings growing on agar plates.

Calculation of the integrated root system age in the different soil layers during the whole growth cycle

From a qualitative viewpoint, ageing of the fine-root system was taken into account because nitrate uptake capacity decreased with increasing root age in the different soil layers (Bhat *et al.*, 1979). Indeed, it well known that due to root system turnover, the root nutrient uptake capacity diminishes with root age because older roots have a lower nutrient uptake capacity than younger roots (Bouma *et al.*, 2001; Eissenstat and Volder, 2005). To further integrate the age effect on the absorbing root biomass, we have used the following formula developed by Gao *et al.* (1998), which was used to calculate the integrated root system age (IRSA) of the whole root system as a function of time. This allowed calculation of the average root age in °Cd produced between two plant ages from d_{i-1} to d_i (where *i* is the *i*th °Cd of root sampling). A given root segment produced during this period of time possesses an average 'birth' date b_i defined as:

$$b_i = (d_{i-1} + d_i)/2 \quad (4)$$

Because roots continue to grow from b_i to $d_{maturity}$, the average root age in °Cd (a_i) relative to the final sampling date ($d_{maturity}$, end of the growth period) corresponds to:

$$a_i = d_{maturity} - b_i = \left[d_{maturity} - (d_{i-1} + d_i)/2\right] \quad (5)$$

Then, IRSA is defined as the sum of the mean age of the root segments produced during that growth period to the total root length:

$$IRSA_i = \sum_{i=1}^{maturity} (a_i \times \Delta l_i / l_{maturity}) \quad (6)$$

where a_i is the average root age of the root produced from plant age d_{i-1} to d_i, Δl_i represents the change in root length from d_{i-1} to d_i and $l_{maturity}$ is the total root length at the end of the growth period (maturity). The IRSA parameter has been previously validated from growth chamber experiments and analyses of data in the literature. It allows characterization of nutrient uptake activity of an entire root system (Gao *et al.*, 1998). Thus, NO_3^- uptake capacities declined with plant age as IRSA increased. However, an older root system with newly formed root segments exhibits a

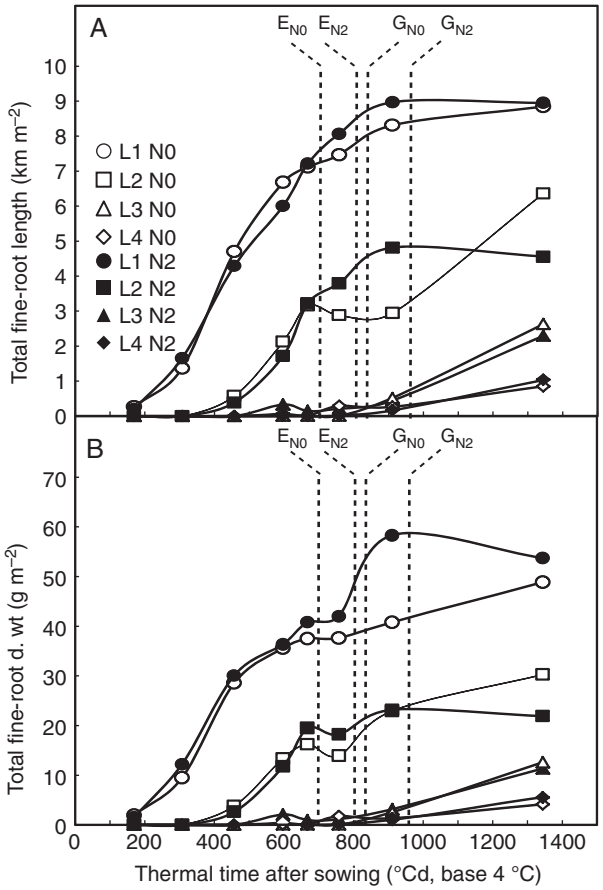

FIG. 3. Variations of estimated root length (A) and dry weight (B) in the different soil layers L1 (0–30 cm), L2 (30–60 cm), L3 (60–90 cm) and L4 (90–120 cm) in a winter oilseed rape crop (*Brassica napus* L. 'Capitol') growing in field conditions under two levels of N fertilization (N0, 0 kg ha^{-1}; N2, 272 kg ha^{-1}) during the whole growth cycle. Dashed lines represent the mean dates for: (stage E) the end of stem elongation and the beginning of handle flower elongation and (stage G2) the start of pod filling for both N fertilization levels, N1 and N2.

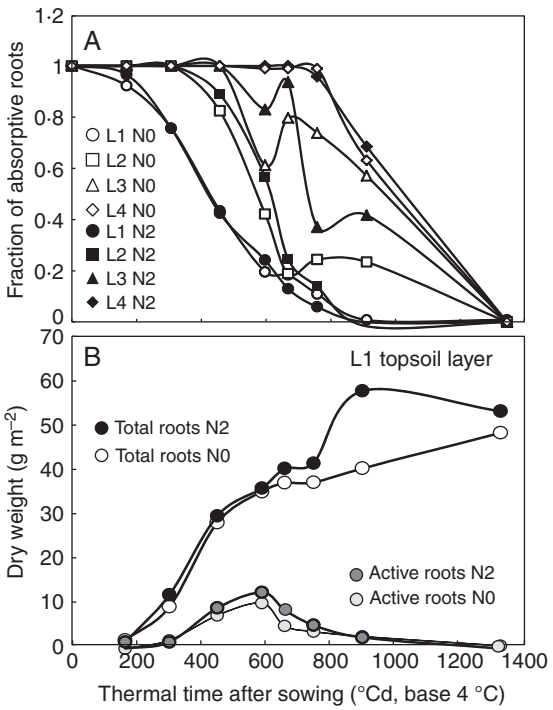

FIG. 4. Variations of the fraction of absorptive roots estimated from IRSA (integrated root system age) during the whole growth cycle in each soil layer for N0 (0 kg ha^{-1}) and N2 (272 kg ha^{-1}) fertilization levels (A) and active absorptive root biomass for N0 and N2 fertilization levels in the L1 (0–30 cm) topsoil layer (B) in a winter oilseed rape crop (*Brassica napus* 'Capitol').

low IRSA value that maintains a slow decrease in the nutrient uptake rate.

Calculation of the active absorbing root biomass based upon the IRSA parameter in the different soil layers during the whole growth cycle

Assuming that the lowest value of the IRSA parameter (young root segments) for each soil layer corresponds to full nitrate uptake capacity (100 %), while the highest IRSA value (old root segments) was reached for absorption equal to zero (Fig. 4A), the active absorbing root fraction is:

$$RF_i = 1 - (IRSA_i/IRSA_{maturity}) \quad (7)$$

where $IRSA_i$ and $IRSA_{maturity}$ are IRSA values at the ith °Cd of root sampling and the final sampling date (maturity), respectively. Then, the active root biomass (ARB) involved in nitrate absorption within the different soil layers during the whole growth cycle is calculated according to:

$$ARB_i = RF_i \times DW_{root,i} \quad (8)$$

As input values of ARB were collected at different dates in the field from root impacts, linear interpolation was chosen between discrete values of the root absorbing biomass throughout the growth cycle. These root biomass values were used as input variables in eqn (1) to run the model.

How to account for soil nitrate heterogeneity caused by fertilization effects?

In our estimation of the active absorbing root biomass, we have also taken into account heterogeneous nitrate supply due to fertilization applications on the root's lifetime (nitrogen fertilization management is given in Table 1). Indeed, applications of N fertilizer in treatments N1 and N2 during the bolting period result in heterogeneous nitrate concentration in the first soil layer (0–30 cm). As N fertilizer was mainly taken up by plant roots in the topsoil layer (0–30 cm, Fig. S2), it was assumed that fertilization increases the root's lifetime and then maintains ARB for a longer time, whereas lack of fertilization induced accelerated ageing of the root system and reduced the active absorbing root biomass.

Model implementation and experimental data for running the model

The functional part of this structure–function mechanistic model of N uptake was programmed using the modelling software Model Maker (Cherwell Scientific) as described by Le Deunff and Malagoli (2014). The root structural data needed to run the model were estimated separately according to the calculations above and

TABLE 1. *Dates and amounts of nitrogen fertilization applied to winter oilseed rape derived from the INRA-database in Grignon (Gosse et al., 1999; http://www-egc.grignon.inra.fr/applis/ecobilan/eco.html): N0, no fertiliser applied; N1 and N2, fertilizer applied*

N application date	Thermal time (°Cd)	N0 (kg N ha^{-1})	N1 (kg N ha^{-1})	N2 (kg N ha^{-1})
09/12/1994	45	–		49
02/20/1995	787	–	78	78
03/15/1995	815	–	57	107
03/29/1995	844	–		38
Total N amount		**0**	**135**	**272**

then introduced as input variables in eqn (1) to run the model. The other input variables such as soil nitrate concentrations, temperature and PAR as well as measured outputs in the field (crop biomass and nitrogen content) needed to run the model were obtained from the INRA oilseed rape database of experiments carried out at Grignon/Châlons/Laon/Reims (http://www-egc.grignon.inra.fr/applis/ecobilan/eco.html). Experimental details can be found in Gosse *et al.* (1999). Soil nitrate concentrations were monitored in four different soil layers (0–30, 30–60, 60–90 and 90–120cm) with and without plants every 2–3 weeks during the growth cycle (for details see Gabrielle *et al.*, 1998*a*). Figure S2 represents the soil nitrate concentrations in the different soil layers along the soil profiles for N0 fertilization with and without plants.

RESULTS

In the topsoil layer, 60–90 % of the whole root system is set before elongation of inflorescence

Time-courses of the total fine-root length (lateral roots) in the different soil layers for both N0 and N2 treatments from field experimental data are presented in Fig. 3 (to simplify presentation, data for the N1 treatment are not shown). Total fine-root length and DW were very similar in the different soil layers. Moreover, N treatments (N1, 0 kg N ha^{-1}; N1, 135 kg N ha^{-1}; N2, 272kg N ha^{-1}) had no significant effect on the final root length and DW. The fine-root length in the 0–30 cm (L1) and 30–60 cm (L2) soil layers at the end of the bolting period (700 and 815 °Cd), just before inflorescence elongation, represented 57 and 88 % of the total root length and DW for N0 and N2 fertilization, respectively (Fig. 3A, B). After the second and third applications of N fertilizer during the bolting period (Table 1), N2 treatments resulted in a significant increase in the root growth rate in the L1 soil layer and to a lesser extent in the L2 soil layer compared with N0 treatment (Fig. 3A). However, at the pod mid-filling stage (1344 °Cd, G2 stage according to the phenological calendar established by the Bayer, BASF, Ciba and Hoechst companies) no difference in total root length was observed between N0 and N2 treatments in both soil layers. At this stage roots present in topsoil layers represented 75–88 % of the total root length for N0 and N2 treatments (Fig. 3A).

Changes in root nitrate uptake capacity as the root ages

Because nitrate uptake capacity diminishes with root age (Bhat *et al.*, 1979; Eissenstat and Volder, 2005) and is not uniform along the root axes (Clarkson *et al.*, 1968; Lazof *et al.*, 1992; Colmer and Bloom, 1998; Sorgona *et al.*, 2011) we have introduced in the model the method of Gao *et al.* (1998) to integrate root system age (IRSA) to estimate the active root absorbing biomass as the root ages (Fig. 4). In the topsoil layer (0–30 cm), the estimated active root biomass (ARB) derived from IRSA declined very rapidly for both N0 and N2 fertilization levels in the different soil layers (Fig. 4A). Because age of the root segments depends on their date of appearance and the root growth rate during the growth cycle, IRSA is responsive to the age of the root segments of the whole root system (Fig. S3). Hence, the decline in ARB was not uniform (Fig. 4A), and this led to a dramatic decrease (80 %) of total fine-root biomass contributing to N uptake for both N0 and N2 fertilization levels in the topsoil layer (Fig. 4B). Therefore, this ARB was used as input variable to run the model.

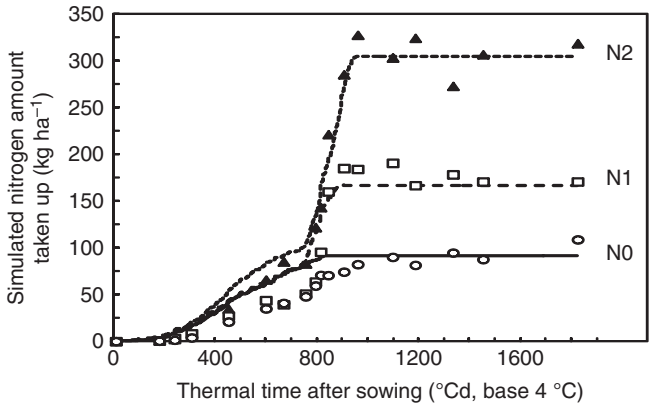

FIG. 5. Simulated (line) and measured (plain symbols) amounts of total nitrogen taken up by a winter oilseed rape crop (*Brassica napus* L. 'Capitol') under three N fertilization levels (N0, 0 kg ha^{-1}; N1, 135 kg ha^{-1}; N2, 272 kg ha^{-1}).

Simulation of N taken up during the whole growth cycle by the model

The simulated course of nitrate taken up under the N0, N1 and N2 fertilization levels is shown in Fig. 5. Predicted values of N exported by the crop match well with measured values, whatever the N fertilization level. Along the same lines, the dynamics of N taken up agreed well between observed and simulated data for the N1 and N2 treatments but were slightly overestimated for the N0 treatment during the first 600 °Cd after sowing. This results from an early start to the simulated N uptake rather than a larger N uptake from 0 to 600 °Cd. Indeed, simulated accumulation of nitrogen in crops parallels measured N taken up by winter oilseed rape.

Effects of environmental and in planta *factors on N uptake regulation*

Application of endogenous and environmental regulation led to a decrease in the unregulated nitrate uptake for N0 and N2 treatments by 54 and 83 %, respectively (Fig. 6A). Among the factor effects, when both day–night and temperature effects were taken into account there was a decrease of 23–30 % in the unregulated nitrate uptake for N0 and N2 fertilization levels (Fig. 6A). Furthermore, a closer of examination of the

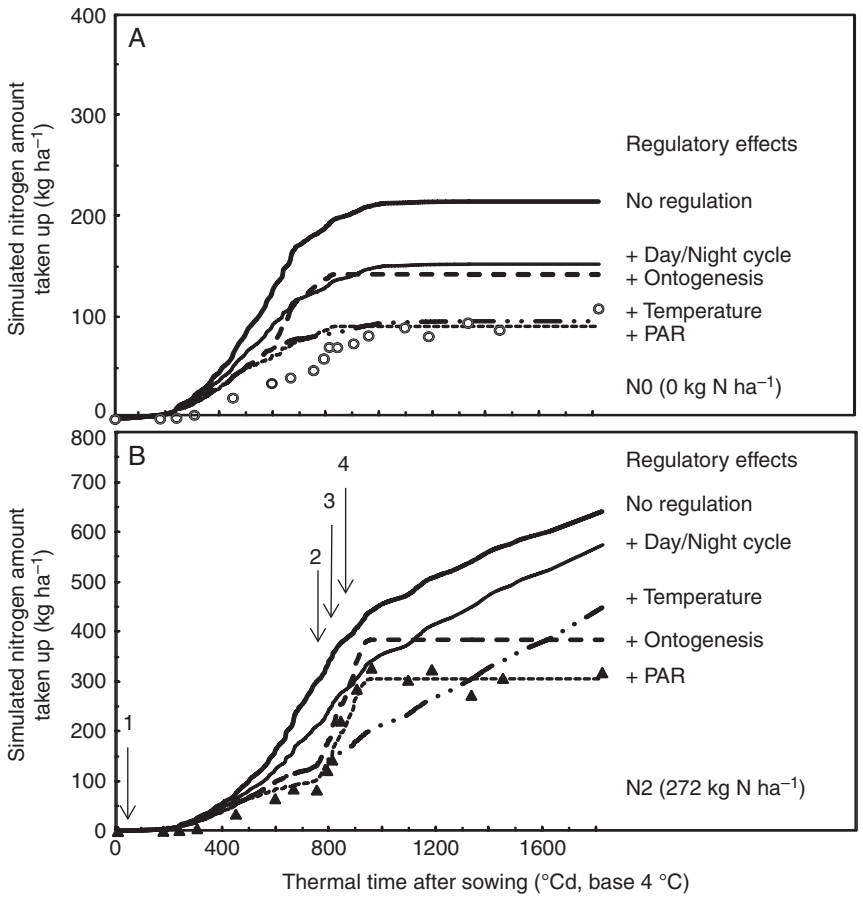

FIG. 6. Simulated (line) amounts of total nitrogen taken up by a winter oilseed rape crop (*Brassica napus* 'Capitol') when day/night, temperature, ontogenesis and PAR effects are cumulatively added under N0 (A) (0 kg ha^{-1}) and N2 (B) (272 kg ha^{-1}) fertilization levels. Symbols refer to measured data derived from the INRA winter oilseed rape database in Grignon (France). (1: 49 kg ha^{-1}; 2: 78 kg ha^{-1}; 3: 107 kg ha^{-1}; 4: 38 kg ha^{-1}). 1 to 4, times of N fertilization application for N2 treatments (see Table 1).

relationship between nitrate influx rate and soil temperature highlighted that temperature was the driving variable explaining variations in the nitrate influx rate during autumn and winter (from 0 to 600 °Cd, $R^2 = 0{\cdot}85$; $P < 0{\cdot}001$), whereas no correlation was established beyond 600 °Cd (Fig. S4). For the N0 and N2 treatments during spring, addition of the ontogenesis effect strongly reduced the unregulated nitrate uptake by 83 and 42 %, respectively (Fig. 6A, B). Thus, adding the ontogenetic effect multiplied nitrate uptake to a variable extent during stem and inflorescence elongation between the D1 and F2 stages for all fertilization levels (Fig. 6A, B). Note that this effect allows shaping of the overall pattern of simulated N taken up during the critical period between D1 and F2 (Fig. 6A). Finally, introducing the PAR effect had the smallest effect on reducing unregulated nitrate uptake during the growth cycle (Fig. S5). The unregulated nitrate uptake finally decreased by 88 and 54 % when all factors were added for the N0 and N2 treatments, respectively (Fig. 6A, B).

Simulated relative contribution of the different soil layers in root N acquisition

Whatever the N fertilization levels, model outputs show that N accumulated in crops is derived substantially from N provided by the 0–30 cm topsoil layer and, to a lesser extent, from the 30–60 cm layer (Fig. 7). Hence, the contribution of the 0–30 cm soil layer to N acquisition ranges from 100 % (when the topsoil layer is the only colonized soil layer at the beginning of the growth cycle) to 71 % (when all soil layers were explored by the root for the N0 fertilization level; Fig. 7A). The decrease in the contribution of the 0–30 cm soil layer is concomitant with the increase in the contribution of the lower 30–60 cm soil layer (up to 19 % of the total N accumulated in crops) due to colonization by roots along the soil profile. Deeper soil layers (60–90 and 90–120 cm) contributed small amounts to crop N accumulation (<10 % at harvest; Fig. 7A). Late addition of N fertilizer (see arrows 2, 3 and 4 in Fig. 7B) led to an improved contribution of the 0–30 cm topsoil layer (90 %), whereas the contribution of the lower soil layers (30–60 and 60–90 cm) to N acquisition was significantly decreased when compared with the N0 fertilization level: only 5·3 and 3·5 % of the total N contribution was derived from the 30–60 and 60–90 cm layers, respectively (Fig. 7A, B).

Simulation of the dynamics of N-NO_3^- influx in each soil layer throughout the growth cycle

Time-courses of simulated N-NO_3^- influx throughout the growth cycle were similar for both N fertilization levels

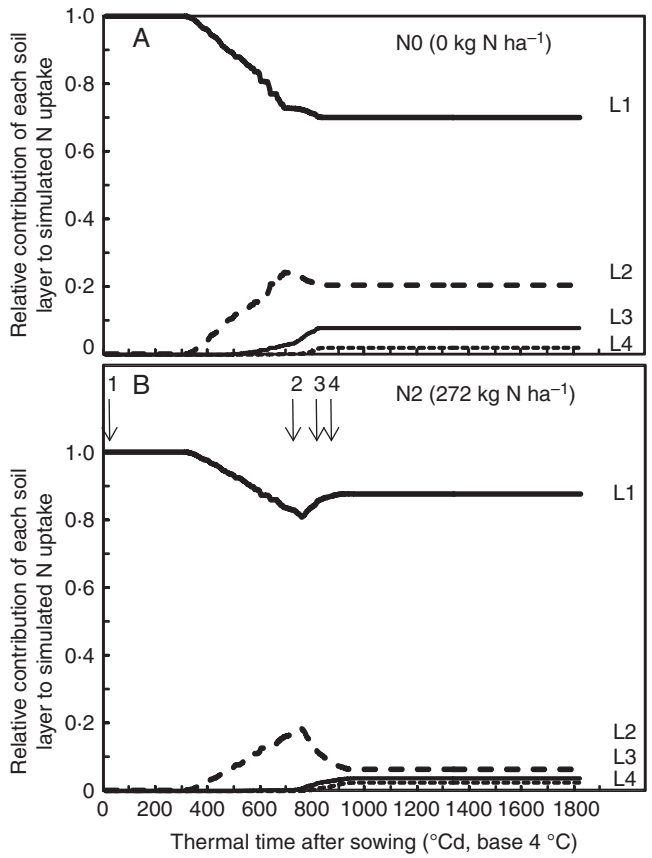

FIG. 7. Simulated relative contribution of each soil layer (L1, 0–30 cm; L2, 30–60 cm; L3, 60–90 cm; L4, 90–120 cm) to N taken up by a winter oilseed rape crop (*Brassica napus* L. 'Capitol') under N0 (0 kg N ha^{-1}) (A) and N2 (272 kg N ha^{-1}) (B) fertilization levels. Arrows correspond to applications of N fertilizer for the N2 fertilization level (1: 49 kg ha^{-1}; 2: 78 kg ha^{-1}; 3:107 kg ha^{-1}; 4: 38 kg ha^{-1}). 1 to 4, times of N fertilization application for N2 treatment (see Table 1).

(Fig. 8). Indeed, evolution of simulated N-NO_3^- influx showed a three-phase pattern. From sowing to 700 °Cd (beginning of extension of floral handle; from D2 to E stage according to the phenological calendar established by the Bayer, BASF, Ciba and Hoechst companies), simulated N-NO_3^- influx decreased dramatically from about 1000 to 200 μmol NO_3^- root d. wt^{-1} 100 $°d^{-1}$ (Fig. 8A, B). Then, simulated N-NO_3^- influx was largely increased until 800 and 900 °Cd for the N0 and N2 fertilization levels, respectively. This corresponds to the mid-flowering stage (stage F2). However, the extent of the increase depended mainly on N fertilization levels. Indeed, simulated N-NO_3^- influx was increased to about 800 and 2500 μmol NO_3^- root d. wt^{-1} 100 $°d^{-1}$ for the N0 and N2 fertilization levels, respectively (Fig. 8A, B). Finally, simulated N-NO_3^- influx dropped sharply and stopped by 1100 °Cd (pod filling; between stage G2 and G3). Note that patterns of simulated N-NO_3^- influx were similar among all soil layers (0–30, 30–60, 60–90 and 90–120 cm) for both N fertilization levels (Fig. 8A, B). Moreover, except for larger values of simulated N-NO_3^- influx in the 0–30 cm topsoil layer at the beginning of the growth cycle for both N fertilization levels, simulated N-NO_3^- influxes were in the same range during the growth cycle, especially for the N2 fertilization level (Fig. 8B).

Simulation of N amounts taken up according to fertilization level and root growth in each soil layer during the growth cycle

Simulated nitrogen amounts taken up in each soil layer were produced from simulated N-NO_3^- influx (i.e. root uptake function, expressed as μmol N-NO_3^-. g^{-1} root d. wt 100 $°Cd^{-1}$) multiplied by estimation of ARB (i.e. root structure, expressed as g m^{-2}) in each soil layer. Simulations of N amounts taken up in each soil layer for both N fertilization levels are presented in Fig. 8(A, D). A logarithm-based expression was chosen to better represent the difference in magnitude of N uptake between each N fertilization level. Model outputs showed that the simulated nitrogen amounts taken up in each soil layer can be characterized by (1) the date of the beginning of N uptake, (2) the maximal N uptake and (3) the duration of the N absorption period (Fig. 8C, D). Although the potential nitrate influx was similar in the different soil layers (Fig. 8A, B), the amount of N taken up depends on the time of soil layer root foraging, ARB within each soil layer and nitrate availability. Accordingly, when no fertilizer was applied, the topsoil layers (0–30, 30–60 cm) contribute massively to N uptake (Fig. 8C). Absorption is driven mainly by the mineralization process and the front of nitrate lixiviation, as shown in Fig. S1. The late application of N fertilizer in the N2 treatment (arrows 2, 3 and 4) induced a biphasic pattern in N taken up within the topsoil layers and increased by one order of magnitude the N taken up compared with the N0 treatment (Fig. 8D).

DISCUSSION

Root life span is a critical variable for simulation of N uptake

As previously shown by Barraclough (1989*a*), compared with annual species such as wheat and maize, 70–80 % of the root length of winter oil seed rape is developed from the sowing (autumn) to the mid part of the bolting period. This means that root and shoot growth are not concomitant and that maximum N uptake (growth stage E, bolting period) occurs when full root growth is almost achieved. Hence, root ageing must be taken into account to accurately estimate ARB during the bolting period from a nutrition viewpoint (Gao *et al.*, 1998; Eissenstat and Volder, 2005; Chen and Brassard, 2013).

The calculation of IRSA, which takes into account the age of the root segments within the whole root system, appears as a key variable because it has been shown that young roots absorb more nitrate than older roots (Edwards and Barber, 1976; Bhat *et al.*, 1979; Colmer and Bloom, 1998; Gao *et al.*, 1998). Moreover, nitrate uptake diminishes along the root axes from the apical part to the basal part (Cushman, 1984; Clarkson, 1988, 1993; Yanai, 1994; Sorgona *et al.*, 2011). The main advantage of using IRSA is that it establishes a link between the root structure and absorptive function because it allows assignment of a root absorption capacity at a specific age of the root. However, the main drawback comes from the fact that this variable does not take into account the effect of a high or low nitrate supply, provided by fertilization or nitrate-rich patches, on root ageing. Indeed, N application may act on the extension or acceleration of root ageing and may increase or decrease N uptake capacities. We assumed that N fertilization reduces acceleration of root ageing because it extends the root functional capacity and delays the flowering date (Le Deunff and Malagoli, 2014).

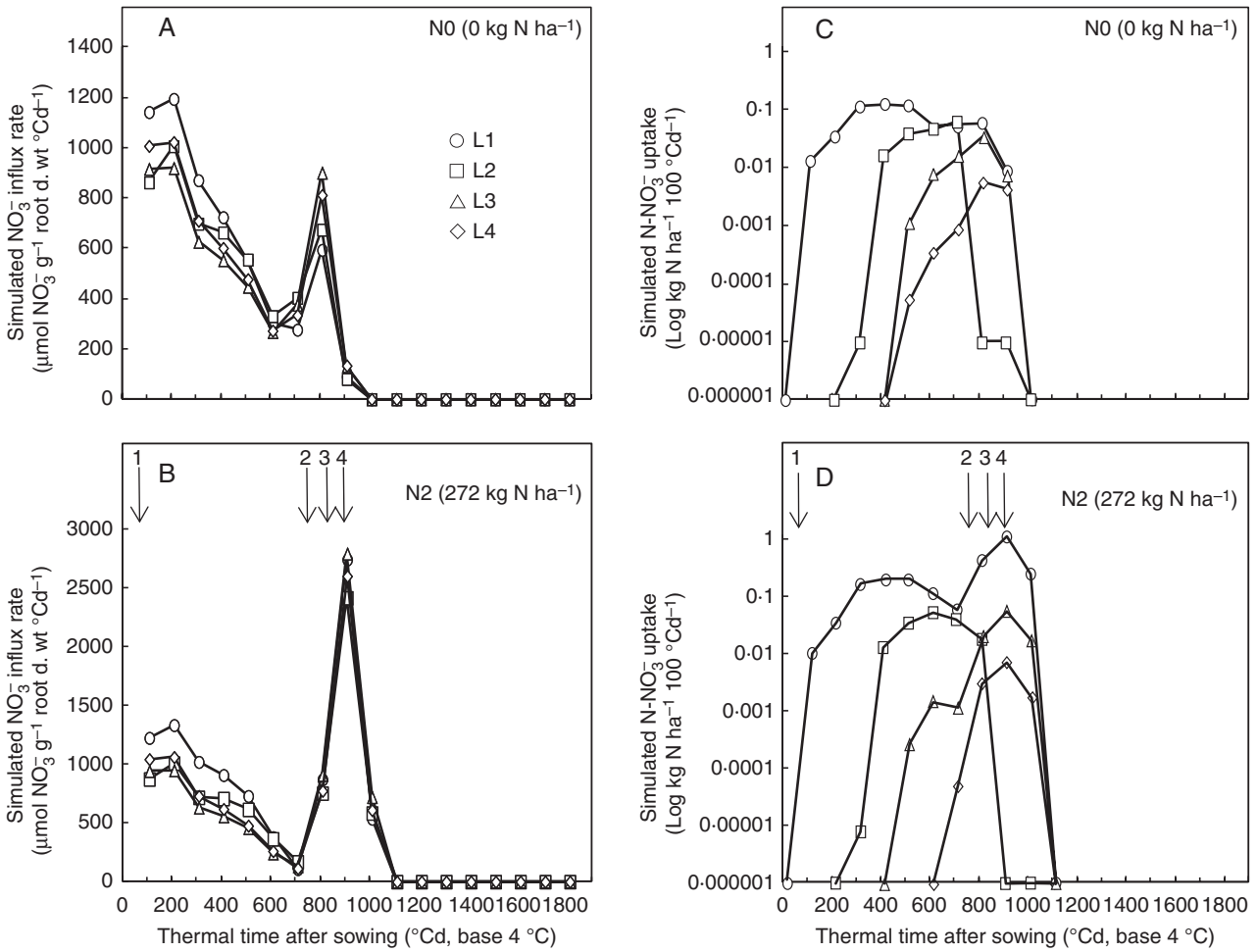

FIG. 8. Simulated NO_3^- influx rate (A, B) and N-NO_3^- uptake during the growth cycle (B, D) in a winter oilseed rape crop (*Brassica napus* 'Capitol') under N0 (0 kg ha^{-1}, top) and N2 (272 kg ha^{-1}, bottom) fertilization levels in each soil layer (L1, 0–30 cm; L2, 30–60 cm; L3, 60–90 cm; L4, 90–120 cm). Simulated N-NO_3^- uptake results from the simulated NO_3^- influx rate and root growth (note the logarithmic scale). Arrows correspond to applications of N fertilizer for the N2 fertilization levels (1: 49 kg N ha^{-1}; 2: 78 kg N ha^{-1}; 3: 107 kg N ha^{-1}; 4: 38 kg N ha^{-1}). 1 to 4, times of N fertilization application for N2 treatment (see Table 1).

This is why the lifetime of fine roots has been artificially prolonged in the 0–30 cm topsoil layer where most of the N applied by fertilization was taken up (Fig. S2). Because nitrate influx reached its maximum value during the bolting period (ontogenetic effect, Fig. 8), it was unlikely that functional compensation ('split root effect') in nitrate uptake could occur at this stage. The extension of the root's lifetime in the first soil layer strongly improved the simulation for N1 and N2 treatments. The results point to the pertinence of IRSA and demonstrate that IRSA calculations in annual and biannual species should be improved by integrating N fertilization effects on the reduction or acceleration of root segment age.

How can similar root length and biomass at the end of the whole growth cycle for all fertilization treatments be explained?

Under field conditions, modelling of nitrogen effects on root formation has often resulted in no significant difference in root length and dry matter, although N content of shoots and roots varies by up to a factor of three among N fertilization levels (Barraclough 1989*a*; Gabrielle *et al.*, 1998*a*, *b*; Kage *et al.*, 2000; Albert, 2008). These estimates of fine-root length and biomass in response to nitrate availability do not agree with physiological experiments in the laboratory. Indeed, it is commonly observed that heterogeneous nitrate supply induces root proliferation in the nitrate-rich patch (Drew, 1975; Drew and Saker, 1975; Robinson, 1996, 2005; Scheible *et al.*, 1997; Zhang *et al.*, 1999), whereas a highly homogeneous nitrate supply induces inhibition of lateral root growth (Zhang *et al.*, 1999; Remans *et al.*, 2006; Le Ny *et al.*, 2013). The dual pathway of root branching has been proposed to explain this paradoxical effect induced by local and systemic signals (Stitt & Scheible, 1998; Zhang *et al.*, 1999; De Kroon *et al.*, 2009). In winter oilseed rape, the lack of a significant effect on total fine-root length and root DW can be explained by a combination of two main factors. At first, 70–88 % of the whole root system develops in the L1 (0–30 cm) and L2 (30–60 cm) topsoil layers before the large N demand for growth resulting from the bolting period and inflorescence expansion. Hence, N fertilization effects will only be observed on growth of the remaining 30 % of the whole root system. At this developmental stage, the root elongation rate declined in the plough layer (L1 and L2) and increased mainly at the other deeper layers (L3 and L4). Secondly, SRL increases with increasing external nitrate

concentration, meaning that roots of equivalent lengths must be heavier under high fertilization than those under low N fertilization level as observed in the field experiments of Barraclough (1989*b*). In our experiment, the similar fine-root DW observed under N0 and N2 fertilization treatments is probably due to an underestimation of the SRL difference between low and high external nitrate concentrations. Indeed, the lack of strong mechanical constraints on the seedlings roots growing on agarose gel probably resulted in an underestimation of the SRL allometric law.

Why is the thermodynamic formalism of the Flow–Force interpretation more suitable to model nitrate transport at the whole plant level throughout the growth cycle?

One of the main problems facing agronomists is how to predict the uptake of nitrogen under field conditions through mechanistic models originating from knowledge acquired in laboratory studies with tracers ^{15}N and ^{13}N. In general, the nitrate isotherms obtained in controlled conditions allow us to establish one or two velocity equations based on the Enzyme–Substrate interpretation of nitrate uptake isotherms, which are then used to model N uptake (Barber, 1995; Peuke and Kaiser, 1996; Le Bot *et al.*, 1998; Ma *et al.*, 2008). However, there are at least two main pitfalls to this approach.

First, the velocity equations are used as reference throughout the growth cycle under field conditions where changes in climatic environment are the rule. This means that the N uptake models based upon velocity equations are inevitably forced by some parameters of the models to match measured N taken up (Ma *et al.*, 2008). The values of such parameters are derived from laboratory studies and it is likely that they vary largely in response to climatic variations and/or *in planta* regulations. Such variations are not taken into account in most of the models including the Enzyme–Substrate interpretation of nitrate uptake isotherms. Hence, as shown by the model outputs, the temperature effect decreases unregulated nitrate uptake by 30 %, whatever the levels of applied fertilization: 0 and 272 kg N ha^{-1}. In fact, temperature appears to be one of the main factors alongside the day–night cycle that is involved in the reduction in nitrate uptake during autumn and winter, as revealed by the significant correlation found between nitrate influx and soil temperature (Fig. S4). This result strengthens the thermodynamic formalism of Flow–Force theory (Thellier, 1970, 1971, 2012; Thellier *et al.*, 2009) over the velocity formalism of the Enzyme–Substrate interpretation (Epstein, 1966, 1972). Indeed, the Flow–Force approach accounts for the driving force on ion transport based on the gradient of electrochemical potential: this is more satisfying from a thermodynamic viewpoint for modelling root nitrate uptake (Thellier, 1970, 1971, 1973). Hence, temperature is one of the parameters in the equation of ion flux in the Flow–Force theory ($J(NO_3^-)_{ext} = RT\lambda NO_3^-$ ln $[NO_3^-]_{ext}$) used to build the model (see our companion paper, Le Deunff and Malagoli, 2014), whereas temperature is not taken into account in the Michaelis–Menten equation of the enzyme-substrate interpretation of nitrate isotherms [$I = V_{max}.[NO_3^-]_{ext}/K_m + [NO_3^-]_{ext}$, where V_{max} is the maximum influx rate (in μmol nitrate h^{-1} g^{-1} root DW) and K_m is the apparent affinity constant (in μM)].

Secondly, structural and molecular studies of root system functioning and architecture from the plant model *Arabidopsis* have revealed that we have to deal with the structural heterogeneity of the mature root cell layers associated with functional heterogeneity of the nitrate transporters. Indeed, the catalytic structure of the mature root for nitrate transport is more complex than previously supposed given that at least four families of transporters (*NRT2*, *NRT1*, *NAXT* and *CLC*) are located in series and/or parallel in plasma and tonoplast membranes of the root cellular layers (Guo *et al.*, 2002; Nazoa *et al.*, 2003; Remans *et al.*, 2006; Girin *et al.*, 2007; Monachello *et al.*, 2009; Segonzac *et al.*, 2011; Feng *et al.*, 2011). Therefore, the symplastic pathway that was used to justify the implicit assumption of a homogeneous root cell structure restricted to the epidermis is no longer valid (Clarkson, 1988, 1993; Crawford and Glass, 1998; Glass, 2007). This explains why over two decades velocity equations of the Enzyme–Substrate interpretation failed to reconcile influx kinetic behaviour with physiological and mutant analyses of nitrate transporters (Forde and Clarkson, 1999; Touraine *et al.*, 2001; Filleur *et al.*, 2001; Liu and Tsay, 2003; Li *et al.*, 2007). Accordingly because the Flow–Force interpretation infers neither the hypothetical cellular processes within the root cell layers nor the type of carriers involved, it appears more in agreement with recent molecular studies.

Flow–Force transformation: an alternative approach to model the kinetics of ion absorption

As previously reported, in most cases linearization of ion isotherms carried out from experimental literature data using the semi-logarithmic coordinates ($\log_{[NO3-]}$; $J_{[NO3-]}$) led to a linear approximation for the low external concentrations corresponding to mechanism I whereas non-linear behaviour was observed for larger external concentrations (>1 mM typically) corresponding to mechanism II (Thellier, 1970, 1973, 2012). Whereas a dual phase in nitrate isotherms is observed after semi-logarithmic transformation in different species such as barley and spruce (Siddiqi *et al.*, 1990; Kronzucker *et al.*, 1995), in studies of Brassicaceae (such as *Arabidopsis thaliana* and *Brassica napus*) linearization of experimental data points over the whole range of external nitrate concentrations (0–10 mM) is often observed (see Fig. S6). These variations in nitrate isotherms in semi-logarithmic coordinates are surprising. Calcium signalling may be responsible for such variable results between species and experiments. Indeed, calcineurin B-like (*CBL*)-interacting protein kinase (*CIPK*) signalling is specifically involved in gene expression regulation of nitrate transporters at high external nitrate concentrations and *cipk8* and *cipk23* mutants showed a flattening in *NRT1·1* and *NRT2·1* gene expression (Ho *et al.*, 2009; Hu *et al.*, 2009). Note also that the large external concentrations used in laboratory experiments (>10 mM) are often beyond the maximum nitrate concentration observed in soil in field conditions after fertilizer applications and are not biologically relevant (Wolt, 1994; Miller *et al.*, 2007). Hence, together these results question the transition between the linear and non-linear behaviour of nitrate isotherms in semi-logarithmic coordinates. Indeed, as previously observed for potassium isotherms, the second phase is flattened by calcium treatments (Epstein and Leggett, 1954; Thellier, 1970, 1973; Ayadi *et al.*, 1974) and we know today that *CBL1* and *CIPK23* proteins are also involved in the regulation of the potassium transporter *AKT1* (Xu *et al.*, 2006).

The model is driven not only by soil nitrate supply: day–night and ontogenetic regulations on nitrate influx matter

Although the model seems to be driven only by root nitrate supply, nitrate uptake is also limited by the daily and ontogenetic growth of the shoots (*in planta* regulations). Indeed, the effects of the day–night and ontogenetic cycles on nitrate uptake regulation resulted from pleiotropic effects. These effects operate at two scales of time and space: they combine (1) the rate of transpiration and translocation during the long-distance of transport signalling molecules between the shoots and roots, (2) the energetic status in the roots (sugar availability) and (3) a combination of N or nitrate signalling for growth associated with N status (Hansen, 1980; Le Bot and Kirby, 1992; Delhon *et al.*, 1995, 1996; Macduff *et al.*, 1997).

Thus, daily accumulation of N, calculated by integrating the influx of nitrate over a period of 24 h and nitrate concentration, depends on external nitrate concentrations (see Le Deunff and Malagoli, 2014). Moreover, daily accumulation of shoot dry weight was also correlated with daily ^{15}N accumulation during the increase in nitrate availability as indicated by seedling experiments (Fig. S7), suggesting that nitrate signal drove the shoot N and C demand for growth. The result was in line with previous data of nitrate reductase mutants in tobacco (Scheible *et al.*, 1997) and recent data in oil seed rape demonstrating that nitrate signal is essential for the shoot growth independently of nitrate reduction and assimilation (Le Ny *et al.*, 2013; Leblanc *et al.*, 2013).

The major ontogenetic effect on nitrate influx regulation occurred during the bolting period between the D1 and F2 stages. Surprisingly, nitrate influx reached is maximum level at stage E corresponding to the maximum of stem extension and the beginning of inflorescence elongation (Le Deunff and Malagoli, 2014). Similarly, recent studies in arabidopsis and maize have revealed a spike in nitrate uptake capacity in the vegetative period before emergence of the floral stem (Nazoa *et al.*, 2003; Garnett *et al.*, 2013). In winter oil seed rape, previous results have shown that this transition between extension of vegetative and reproductive shoot tissues was marked by the appearance of a leaf with a specific shape called leaf α (Netzer *et al.*, 1989). In fact, leaf α defines exactly the transition between the cohort of the stem's leaves and the cohort of the floral handle's leaves and is marked by the beginning of the remobilization processes during the formation of reproductive tissues (Malagoli *et al.*, 2008). Further work in our laboratory has also shown that between the D1 and F2 stages the total amino acids decreased in the phloem sap collected at the stem basis. In particular, the amount of glutamine (Gln) drops sharply (Beuve *et al.*, 2004). This would explain the alleviation of nitrate influx during vegetative growth because some amino acids such as Gln are known to downregulate nitrate uptake activity and especially expression of the *BnNRT2·1* nitrate transporter (Vidmar *et al.*, 2000; Nazoa *et al.*, 2003; Beuve *et al.*, 2004; Leblanc *et al.*, 2013). Indeed, it is well established that the *NRT2·1* nitrate transporter is mainly involved in root N uptake (Okamoto *et al.*, 2003; Garnett *et al.*, 2013; Le Ny *et al.*, 2013; Leblanc *et al.*, 2013). Furthermore, the increase in nitrate influx runs in parallel to the expansion of leaf surface area and photosynthesis that favour sugar allocation to the root and ATP production via H^+-ATPase. H^+-ATPase energizes the transport of ions such as nitrate (Lejay *et al.*, 1999, 2003, 2008; Sorgona *et al.*, 2011). Then, nitrate influx declined from E to F2 stage during the extension of the inflorescence (Nazoa *et al.*, 2003; Le Deunff and Malagoli, 2014). Given the low levels of phloem amino acids at these developmental stages (Beuve *et al.*, 2004), the reduction in C supply to the root during flowering and seed filling could be the main cause of the decline in root absorption (Lejay *et al.*, 2003, 2008). Taken together, these data suggest that the developmental regulation of nitrate uptake during ontogenesis probably reflects the C and N regulation of the *NRT2·1* promoter associated with changes in phloem sap composition throughout the growth cycle (Nazoa *et al.*, 2003; Girin *et al.*, 2007).

In conclusion, the model presented was able to predict satisfactorily both the final nitrogen exported by a winter oilseed rape crop and the dynamics of nitrate uptake during the growth cycle. This mechanistic model relies on a structure–function approach. From a functional viewpoint, N uptake derives from a new conceptual framework that combines a Flow–Force interpretation of nitrate uptake kinetics with environmental and *in planta* effects on nitrate influx regulation (Le Deunff and Malagoli, 2014). In brief, the novelty of this model is that it replaces the use of reference influx isotherms as commonly presented in most current agronomic models (Barber, 1995; Tinker and Nye, 2000; Ma *et al.*, 2008) by oscillations of nitrate influx in response to endogenous and *in planta* factors. From a structural viewpoint, the estimation of ARB has been improved compared with that by Malagoli *et al.* (2004). In fact, root biomass was estimated from a combination of field root impacts and SRL to account for variations in nitrate concentration within colonized soil layers. The relationship between structure and function was achieved by introduction of the integrated root system age (IRSA variable) that allows assignment of a root absorption capacity at a specific age of the root and calculation of root biomass contributing actively to nitrate uptake. Thus, ARB depends on a quantitative change through SRL and a qualitative change through high IRSA.

SUPPLEMENTARY DATA

Supplementary data are available online at www.aob.oxfordjournals.org and consist of the following. Figure S1: mean nitrate concentrations in the different soil layers in the absence of plants for the N0 (0 kg N ha^{-1}) fertilization level. Fig. S2: time-course of nitrate concentrations in the topsoil layers for the different fertilization levels in the absence and presence of plants during the whole growth cycle. Fig. S3: time-course of integrated root system age (IRSA) during the whole growth cycle in each soil layer for two fertilization levels. Fig. S4: variations of NO_3^- influx as a function of temperature. Fig. S5: variations of NO_3^- influx as a function of PAR. Fig. S6: kinetic characteristics of nitrate influx and net nitrate absorption adjusted with Epstein or Thellier mathematical transformations in wild-type and *nrt2·1nrt2·2* and *chl1·5* arabidopsis mutant plants. Fig. S7: correlation between daily $^{15}NO_3^-$ absorption and daily dry weight accumulation in the shoot of 7-d-old winter oilseed rape seedlings growing on agar plates and treated with increasing external nitrate concentration from 0·05 to 5 mM.

ACKNOWLEDGEMENTS

This work was supported by the Regional Council of Basse-Normandie. We thank Prof. Eric Reyssat (Laboratoire de Mathématiques N. Oresmes, Université de Caen, France) for his assistance with the mathematics used in the model.

LITERATURE CITED

Albert B. 2008. Architecture racinaire et efficience d'utilisation de l'azote chez deux génotypes de colza cultivés en conditions contrastées d'alimentation azotée. www.bioveg.auf.org/IMG/pdf/S3-C14-Albert.pdf [accessed 17 July 2013].

Ayadi A, Stelz T, Monnier A, Lasssales JP, Thellier M. 1974. Application of an electrokinetic formulation to study of the effect of alcanine-earth cations on the absorption of K^+ ions by *Lemna minor*. *Annals of Botany* **38**: 677–696.

Barber SA. 1995. Nutrient absorption by plant roots. In: Barber SA, ed. *Soil nutrient bioavailability: a mechanistic approach*. New York: Wiley, 49–84.

Barraclough PB. 1989*a*. Root growth and nutrient uptake by field crops under temperate conditions. *Aspect of Applied Biology* **22**: 227–233.

Barraclough PB. 1989*b*. Root growth, macro-nutrient uptake dynamics and soil fertility requirements of a high-yielding winter oilseed rape. *Plant and Soil* **119**: 59–70.

Bhat KKS, Nye PH, Brereton AJ. 1979. The possibility of predicting solute uptake and plant growth response from independently measured soil and plant characteristics VI. The growth and uptake of rape in solutions of constant nitrate concentration. *Plant and Soil* **53**: 137–167.

Beuve N, Rispail N, Laîné P, Cliquet JB, Ourry A, Le Deunff E. 2004. Putative role of gamma-aminobutyric acid (GABA) as a long distance signal in up-regulation of nitrate uptake in *Brassica napus* L. *Plant Cell, and Environment* **27**: 1035–1046.

Bouma TJ, Yanai RD, Elkin AD, Hartmond U, Flores-Alva DE, Eissenstat DM. 2001. Estimating age-dependent costs and benefits of roots with contrasting life span: comparing apples and oranges. *New Phytologist* **150**: 685–695.

Brouder SM, Volenec JJ. 2008. Impact of climate change on crop nutrient and water use efficiencies. *Physiologia Plantarum* **133**: 705–724.

Chen HYH, Brassard BW. 2013. Intrinsic and extrinsic controls of fine root life span. *Critical Review of Plant Science* **32**: 151–161.

Clarkson DT. 1988. Movements of ions across roots. In: Baker DA, Hall JL, eds. *Solute transport in plant cells and tissues*. Harlow: Longman Scientific and Technic, 251–304.

Clarkson DT. 1993. Roots delivery of solutes to the xylem. *Philosophical Transactions of the Royal Society London B* **341**: 5–17.

Clarkson DT, Sanderson J, Russell RS. 1968. Ion uptake and root age. *Nature* **220**: 805–806.

Colmer TD, Bloom AJ. 1998. A comparison of NH_4^+ and NO_3^- net fluxes along roots of rice and maize. *Plant, Cell and Environment* **21**: 240–246.

Crawford NM, Glass ADM. 1998. Molecular and physiological aspects of nitrate uptake in plants. *Trends in Plant Science* **3**: 389–395.

Cushman J. 1984. Numerical study of some age-dependent parameters in root nutrient uptake. *Plant and Soil* **79**: 123–141.

De Kroon H, Visser EJW, Huber H, Mommer L, Hutchings MJ. 2009. A modular concept of plant foraging behaviour: the interplay between local responses and systemic control. *Plant, Cell and Environment* **32**: 704–712.

Delhon P, Gojon A, Tillard P, Passama L. 1995. Diurnal regulation of NO_3^- uptake in soybean plants I. Changes in NO_3^- influx, efflux and N utilization in the plant during the day/night cycle. *Journal of Experimental Botany* **46**: 1585–1594.

Delhon P, Gojon A, Tillard P, Passama L. 1996. Diurnal regulation of NO_3^- uptake in soybean plants IV. Dependence on current photosynthesis and sugar availability to the roots. *Journal of Experimental Botany* **47**: 893–900.

Drew MC. 1975. Comparison of the effects of a localized supply of phosphate, nitrate, ammonium and potassium on the growth of the seminal root system, and the shoot in Barley. *New Phytologist* **75**: 479–490.

Drew MC, Saker LR. 1975. Nutrient supply and the growth of the seminal root system in barley. *Journal of Experimental Botany* **26**: 79–90.

Edwards JH, Barber SA. 1976. Nitrogen uptake characteristics of corn roots at low N concentration as influenced by plant age. *Agronomy Journal* **68**: 17–19.

Eissenstat DM, Volder A. 2005. The efficiency of nutrient acquisition over the life of a root. In Bassirirad H ed. *Nutrient acquisition by plants: an ecological perspective*, 1st edn. Berlin: Springer-Verlag, 185–212.

Epstein E. 1966. Dual pattern of ion absorption by plant cells and by plants. *Nature* **212**: 1324–1327.

Epstein E. 1972. Nutrient absorption by plants. In: Epstein E, Bloom AJ, eds. *Mineral nutrition of plants: principles and perspectives*, 2nd edn. New York: Wiley, 69–95.

Epstein E, Leggett JE. 1954. The absorption of alkaline earth cations by barley roots: kinetics and mechanism. *American Journal of Botany* **4**: 785–791.

Feng H, Yan M, Fan X, *et al*. 2011. Spatial expression and regulation of rice high-affinity nitrate transporters by nitrogen and carbon status. *Journal of Experimental Botany* **62**: 2319–2332.

Filleur S, Dorbe MF, Cerezo M, *et al*. 2001. Arabidopsis T-DNA mutant affected in Nrt2 genes is impaired in nitrate uptake. *FEBS Letters* **489**: 220–224.

Forde BG, Clarkson DT. 1999. Nitrate and ammonium nutrition of plants: physiological and molecular perspectives. *Advance in Botanical Research* **30**: 1–90.

Gabrielle B, Denoroy P, Gosse G, Justes E, Andersen MN. 1998*a*. Development and evaluation of a CERES-type model for winter oilseed rape. *Field Crops Research* **57**: 95–111.

Gabrielle B, Justes E, Denoroy P. 1998*b*. Modelling of temperature and nitrogen effects on the rooting dynamics of winter oilseed rape. Association française pour l'étude du sol & International Society of Soil Science. *Proceedings of the 16th World Congress of Soil Science on CD-ROM*. ISSS-AISS-IBG-SICS.

Gan Y, Liu L, Cutforth H, Wang X, Ford G. 2011. Vertical distribution profiles and temporal growth patterns of roots in selected oilseeds, pulses and spring wheat. *Crop and Pasture Science* **62**: 457–466.

Gao S, Pan WL, Koening R. 1998. Integrated root system age in relation to plant nutrient uptake activity. *Agronomy Journal* **90**: 505–510.

Garnett T, Conn V, Plett D, *et al*. 2013. The response of the maize nitrate transport system to nitrogen demand and supply across the lifecycle. *New Phytologist* **198**: 82–94.

Gerwitz S, Page E. 1974. An empirical mathematical model to describe plant root systems. *Journal of Applied Ecology* **11**: 773–781.

Girin T, Lejay L, Wirth J, *et al*. 2007. Identification of a 150 bp cis-acting element of the AtNRT2·1 promoter involved in the regulation of gene expression by the N and C status of the plant. *Plant, Cell and Environment* **30**: 1366–1380.

Glass ADM. 2007. The apoplast: a kinetic perspective. In: Sattelmacher B, Horst WJ, eds. *The apoplast of higher plants: compartment of storage, transport and reactions*, 1st edn. Hannover: Springer, 87–96.

Good AG, Shrawat A, Muench DG. 2004. Can less yield more? Is reducing nutrient input into the environment compatible with maintaining crop production? *Trends in Plant Science* **9**: 597–605.

Gosse G, Cellier P, Denoroy P, *et al*. 1999. Water, carbon and nitrogen cycling in a rendzina soil cropped with winter rape: the Châlons oilseed rape database. *Agronomie* **19**: 119–124.

Gregory PJ, George TS. 2011. Feeding nine billion: the challenge to sustainable crop production. *Journal of Experimental Botany* **62**: 5233–5248.

Guo FQ, Wang R, Crawford NM. 2002. The *Arabidopsis* dual-affinity nitrate transporter gene *AtNRT1·1* (CHL1) is regulated by auxin in both shoots and roots. *Journal of Experimental Botany* **53**: 835–844.

Hansen GK. 1980. Diurnal variation of root respiration rates and nitrate uptake as influenced by nitrogen supply. *Physiologia Plantarum* **48**: 421–427.

Herder GD, Isterdael GV, Beeckman T, De Smet I. 2010. The root of a new green revolution. *Trends in Plant Science* **15**: 600–607.

Ho C-H, Lin S-H, Hu H-C, Tsay Y-F. 2009. CHL1 functions as a nitrate sensor in plants. *Cell* **138**: 1184–1194.

Hu HC, Wang Y-Y, Tsay Y-F. 2009. AtCIPK8, a CBL-interacting protein kinase, regulates the low-affinity phase of the primary nitrate response. *Plant Journal* **57**: 264–278.

Kage H, Kochler M, Stützel H. 2000. Root growth of cauliflower (*Brassica oleracea* L. botrytis) under unstressed conditions: measurements and modelling. *Plant and Soil* **223**: 131–145.

King J, Gay A, Sylvester-Bradley R, *et al*. 2003. Modelling cereal root systems for water and nitrogen capture: towards an economic optimum. *Annals of Botany* **91**: 383–390.

Kronzucker HJ, Siddiqi MY, Class ADM. 1995. Kinetics of NO_3^- influx in spruce. *Plant Physiology* **109**: 319–326.

Lazof DB, Rufty TW, Redinbaugh MG. 1992. Localization of nitrate absorption and translocation within morphological regions of the corn root. *Plant Physiology* **100**: 1251–1258.

Leblanc A, Segura R, Deleu C, Le Deunff E. 2013. In low transpiring conditions, uncoupling the BnNrt2·1 and BnNrt1·1 NO_3^- transporters by glutamate treatment reveals the essential role of BnNRT2·1 for nitrate uptake and the nitrate-signalling cascade during growth. *Plant Signaling and Behavior* **8**: e22904.

Le Bot J, Kirby EA. 1992. Diurnal uptake of nitrate and potassium during vegetative growth of tomato plants. *Journal of Plant Nutrition* **15**: 257–264.

Le Bot J, Adamowicz S, Robin P. 1998. Modelling plant nutrition of horticultural crops: a review. *Scienta Horticulturae* **74**: 47–82.

Le Deunff E, Malagoli P. 2014. An updated model for nitrate uptake modelling in plants. I. Functional component: cross-combination of flow–force interpretation of nitrate uptake isotherms, and environmental and *in planta* regulation of nitrate influx. *Annals of Botany* **113**: 991–1005.

Lejay L, Tillard P, Domingo Olive F, *et al*. 1999. Molecular and functional regulation of two NO_3^- uptake systems by N- and C-status of *Arabidopsis* plants. *Plant Journal* **18**: 509–519.

Lejay L, Gansel X, Cerezo M, *et al*. 2003. Regulation of root ion transporter by photosynthesis: functional importance and relation with hexokinase. *Plant Cell* **15**: 2218–2232.

Lejay L, Wirth J, Pervent M, Cross JM-F, Tillard P, Gojon A. 2008. Oxidative pentose phosphate pathway-dependent sugar sensing as a mechanism for regulation of root ion transporters by photosynthesis. *Plant Physiology* **146**: 2036–2053.

Le Ny F, Leblanc A, Beauclair P, Deleu C, Le Deunff E. 2013. In low transpiring conditions, nitrate and water fluxes for growth of *B. napus* plantlets correlate with changes in *BnNrt2·1* and *BnNrt1·1* nitrate transporters expression. *Plant Signaling and Behavior* **8**: e22902.

Li W, Wang Y, Okamoto M, Crawford NM, Siddiqi MY, Glass ADM. 2007. Dissection of the AtNRT2·1:AtNRT2·2 inducible high-affinity nitrate transporter gene cluster. *Plant Physiology* **143**: 425–433.

Liu K-H, Tsay Y-F. 2003. Switching between the two action modes of the dual affinity nitrate transporter CHL1 by phosphorylation. *EMBO Journal* **22**: 1005–1013.

Liu LP, Gan YT, Bueckert RA, Warkentin TD. 2010. Fine root distribution of oilseeds and pulses in semiarid environment. *Crop Science* **50**: 222–226.

Liu LP, Gan YT, Bueckert R, van Rees K. 2011*a*. Rooting systems of oilseed and pulse crops I: Temporal growth patterns across the plant developmental periods. *Field Crop Research* **122**: 256–263.

Liu LP, Gan YT, Bueckert R, van Rees K. 2011*b*. Rooting systems of oilseed and pulse crops II: Vertical distribution patterns across the soil profile. *Field Crop Research* **122**: 248–255.

Lynch JP. 2007. Roots of the second green revolution. *Australian Journal of Botany* **55**: 493–512.

Ma L, Ahuja LR, Bruulsema TW. 2008. Current status and future needs in modeling plant nitrogen uptake: a preface. In: Ma L, Ahuja L, Bruulsema T, eds. *Quantifying and understanding plant nitrogen uptake for systems modeling*. Boca Raton, FL: Taylor and Francis, 1–11.

Macduff JH, Bakken AK, Dhanoa MS. 1997. An analysis of the physiological basis of commonality between diurnal patterns of NH_4^+, NO_3^- and K^+ uptake by *Phleum pratense* and *Festuca pratensis*. *Journal of Experimental Botany* **48**: 1691–1701.

Maertens C. 1987. Minirhizotron observation tubes: methods and applications for measuring rhizosphere dynamics. Madison, WI: American Society of Agronomy.

Malagoli P, Laine P, Le Deunff E, Rossato L, Ney B, Ourry A. 2004. Modeling N uptake in *Brassica napus* L. cv capitol during growth cycle using influx kinetics of nitrate transport systems and field experimental data. *Plant Physiology* **134**: 388–400.

Malagoli P, Meuriot F, Laine P, Le Deunff E, Ourry A. 2008. Modelling nitrate uptake and N dynamics in winter oilseed rape (*Brassica napus* L.) during the growth cycle. In: Ma L, Ahuja L, Bruulsema T, eds. *Quantifying and understanding plant nitrogen uptake for systems modeling*. Boca Raton, FL: Taylor and Francis, 47–69.

Miller AJ, Fan X, Orsel M, Smith SJ, Wells DW. 2007. Nitrate transport and signalling. *Journal of Experimental Botany* **58**: 2297–2306.

Monachello D, Allot M, Oliva S, *et al*. 2009. Two anion transporters AtClCa and AtClCe fufil interconnecting but not redundant roles in nitrate assimilation pathways. *New Phytologist* **183**: 88–94.

Nazoa P, Vidmar JJ, Tranbarger TJ, *et al*. 2003. Regulation of the nitrate transporter gene *AtNRT2·1* in *Arabidopsis thaliana*: responses to nitrate, amino acids and developmental stage. *Plant Molecular Biology* **52**: 689–703.

Netzer MH, Tittonnel ED, Merrien A. 1989. Evénements liés au passage du méristème de l'état végétatif à l'état reproducteur, chez le colza, *Brassica napus*. L. var. *oleifera* Metzg. *Agronomie* **9**: 151–159.

Newman EI. 1966. A method of estimating the total root length in a sample. *Journal of Applied Ecology* **3**: 139–145.

Okamoto M, Vidmar JJ, Glass ADM. 2003. Regulation of *NRT1* and *NRT2* gene families of *Arabidopsis thaliana*: responses to nitrate provision. *Plant, Cell Physiology* **44**: 304–317.

Peuke AD, Kaiser WM. 1996. Nitrate or ammonium uptake and transport and rapid regulation of nitrate reduction in higer plants. In: Lüttge U, Beyschlag W, Büdel B, Francis D, eds. Progress in botany *57*. Berlin: Springer-Verlag, 93–113.

Petersen CT, Jøgensen U, Svendsen H, Hansen S, Jensen HE, Nielsen NE. 1995. Parameter assessment for simulation of biomass production and nitrogen uptake in winter rape. *European Journal of Agronomy* **1**: 77–89.

Remans T, Nacry P, Pervent M, *et al*. 2006. A central role for the nitrate transporter NRT2·1 in the integrated morphological and physiological responses of the root system to nitrogen limitation in Arabidopsis. *Plant Physiology* **140**: 909–921.

Robinson D. 1996. Variation, co-ordination and compensation in root systems in relation to soil variability. *Plant and Soil* **18**: 57–66.

Robinson D. 2005. Integrated root responses to variations in nutrient supply. In: BassiriRad H, ed. *Nutrient acquisition by plants: a ecological perspective*. Berlin: Springer-Verlag, 45–61.

Scheible W, Lauerer M, Schulze E, Caboche M, Stitt M. 1997. Accumulation of nitrate in the shoot acts as a signal to regulate shoot-root allocation in tobacco. *Plant Journal* **11**: 671–691.

Segonzac C, Boyer JC, Ipotesi E, *et al*. 2011. Nitrate efflux at the root plasma membrane: identification of an arabidopsis excretion transporter. *Plant Cell* **19**: 3760–3777.

Siddiqi MY, Glass ADM, Ruth TJ, Rufty TW. 1990. Studies of the uptake of nitrate in barley: I. Kinetics of $^{13}NO_3^-$ influx. *Plant Physiology* **93**: 1426–1432.

Sorgona A, Lupini A, Mercati F, Di Dio L, Sunseri F, Abenavoli MR. 2011. Nitrate uptake along the maize primary root: an integrated physiological and molecular approach. *Plant, Cell and Environment* **34**: 1127–1140.

Stitt M, Scheible W. 1998. Understanding location to shoot and root growth will require molecular information about which compounds act as signals for the plant nutrient status, and how meristem activity and cellular growth are regulated. *Plant and Soil* **201**: 259–263.

Thellier M. 1970. An electrokinetic interpretation of the functioning of biological systems and its application to the study of mineral salts absorption. *Annals of Botany* **34**: 983–1009.

Thellier M. 1971. Non-equilibrum thermodynamics and electrokinetic interpretation of biological systems. *Journal of Theoretical Biology* **31**: 389–393.

Thellier M. 1973. Electrokinetic formulation of ionic absorption by plants samples. In: Anderson WP, ed. *Ion transport in plants.* London: Academic Press, 47–63.

Thellier M. 2012. A half-century adventure in the dynamics of living systems. In: Lüttge U, Beyschlag W, Büdel B, Francis D, eds. *Progress in botany.* Berlin: Springer-Verlag, 57–81.

Thellier M, Ripoll C, Norris V, Nikolic M, Römeheld V. 2009. Solute uptake in plants: flow/force interpretation. In: Lüttge U, Beyschlag W, Büdel B, Francis D, eds. *Progress in botany.* Berlin: Springer-Verlag, 53–68.

Tinker PB, Nye PH. 2000. Solute transport and crop growth models in the field. In: Tinker PB, Nye PH, eds. *Solutes movement in the rhizosphere*, 1st edn. New York: Oxford University Press, 308–371.

Touraine B, Daniel-Vedele F, Forde BG. 2001. Nitrate uptake and its regulation. In: Lea PJ, Morot-Gaudry JF, eds. *Plant nitrogen.* Berlin, Heidelberg: INRA and Springer-Verlag, 1–36.

Vidmar JJ, Zhuo D, Siddiqi MY, Schoerring JK, Touraine B, Glass ADM. 2000. Regulation of high-affinity nitrate transporter genes and high-affinity nitrate influx by nitrogen pools in roots of barley. *Plant Physiology* **123**: 307–318.

Warncke DD, Barber SA. 1974. Root development and nutrient uptake by corn grown in solution culture. *Agronomy Journal* **66**: 514–516

Wolt JD. 1994. Soil solution chemistry: application to environmental science and agriculture. New York: Wiley.

Xu J, Li HD, Chen LQ, *et al*. 2006. A protein kinase, interacting with two calcineurin B-like proteins, regulates K+ transporter AKT1 in Arabidopsis. *Cell* **125**: 1347–1360.

Yanai RD. 1994. A steady-state model of nutrient uptake accounting for newly grown roots. *Soil Science Society of American Journal* **58**: 1562–1571.

Zhang H, Jenning A, Barlow PW, Forde BG. 1999. Dual pathways for regulation of root branching by nitrate. *Proceedings of National Academy of Science USA* **96**: 6529–6534.